Jerusalem Symposium on Quantum Chemistry, May, 1989)

BNL-42831

CONF-8905146--1

BNL--42831

DE89 013568

SUPEREXCHANGE COUPLING MECHANISMS FOR ELECTRON TRANSFER PROCESSES

M. D. NEWTON
Chemistry Department
Brookhaven National Laboratory
Upton, NY 11973 USA

ABSTRACT. Electron transfer matrix elements for electron exchange between various pairs of transition metal complexes in close contact have been calculated and analyzed for a variety of approach geometries for the two reactants. The coupling between the nominal metal ion donor/acceptor sites is achieved by superexchange of the "hole" type arising from ligand-to-metal charge transfer (LMCT), the dominant ligand-field interaction for the electron-donor ligands considered (H_2O, NH_3, and the cyclopentadienide anion). The pronounced variations of H_{if} with geometry are not correlated with the separation distance of the metal ions (between which the direct overlap is negligible) and span the range from non-adiabatic to strongly adiabatic electronic coupling. The values for metallocene/metallocinium redox pairs bracket recently reported experimental values. Analysis of the results using the method of corresponding orbitals demonstrates the validity of an effective 1-electron model for the electron transfer process to within about 10% for the class of systems considered. A higher-order superexchange mechanism was encountered for the $Co(NH_3)_6{}^{2+/3+}$ exchange process, in which the LMCT-driven hole-transport mechanism couples excited local states of the metal ions, which in turn are connected to the corresponding ground states by spin-orbit mixing. This mechanism yields on electronic transmission factor within two orders of magnitude of unity.

1. INTRODUCTION

The kinetics of electron transfer processes are controlled by a number of energetic and dynamical factors involving both nuclear and electronic degrees of freedom [1-4]. While traditional approaches have focused most attention on the activation energy [1,2], with primary application to small molecular reactants in close contact, more recent interest in transfer between widely separated donor and acceptor sites has increasingly focussed attention on the electronic structural aspects of the process [5-9]. Since direct orbital overlap between local donor and acceptor sites becomes negligible if their

separation exceeds a few angstroms, the electronic coupling is typically formulated perturbatively as an indirect process involving virtual intermediate states [2,8,10,11]. In spite of the fact that such superexchange mechanisms are in principle many-electron phenomena, one in general expects a one-electron model to provide a viable approximation for electron transfer processes [6c], in contrast to analogous two-electron superexchange coupling between localized spin sites [12].

While the formulation of superexchange coupling is fairly straight-forward, the multiiplicity of possible "pathways" which arise in complex systems and which may interfere with each other constructively or destructively, often makes quantitative implementation of superexchange schemes quite difficult. Nevertheless, the availability of sophisticated computational techniques for determining electronic structural features of complex molecular systems has made it possible to attempt detailed superexchange analyses for certain redox processes [6c].

In the present paper we illustrate two different types of superexchange coupling associated with electron exchange processes involving coordinated transition metal ions:

$$ML_n^{z+} + ML'^{(z+1)+}_n \longrightarrow ML_n^{(z+1)+} + ML'^{z+}_n \qquad (1)$$

When the redox partners are in contact, good overlap will exist between one or more pairs of ligands (L,L'). Indirect coupling of the nominal donor and acceptor orbitals (taken as the 3d orbitals of the metal ions M,M') can then be facilitated by ligand-metal covalent mixing [6c]. In some cases, this type of supercharge coupling is supplemented by a second type arising from spin-orbit coupling [13,14]. This latter situation will be illustrated for the case of M = Co, L = NH_3 (z=2, n=6).

As noted above, one expects to be able to formulate an electron transfer process within a "one-electron" framework, a consideration of no small importance when it comes to modeling very complex processes as, for example, occur in protein-based systems [8,9] or in photosynthesis [15,16]. In the present paper we will address the validity of the one-electron model from the perspective of results obtained from a computational model which includes all the valence electrons of the two redox partners. In particular, we shall evaluate the electron transfer matrix elements,

$$H_{if} = \int \psi_i H \psi_f d\tau \qquad (2)$$

which couple the initial and final states in the electron transfer process, where H is the full (many-electron) Schroedinger electronic Hamiltonian associated with the reaction partners in their close-contact encounter complex (this precursor complex will be treated as a supermolecule complex in the calculations reported below).

We wish to understand the sensitivity of H_{if} values to the detailed electronic structure of the reactants and to structural variations within the encounter complex, especially the relative orientation of the redox partners and the separation of the nominal donor/acceptor sites (M,M'). Relative to the simple model in which H_{if} is taken as a one-electron resonance integral between spherical donor and acceptor orbitals, so that the only structural dependence is an exponential dependence on donor/acceptor separation, we shall find a much richer pattern in which through-bond (TB) and through-space (TS) factors control the variations of H_{if} with orientation. These variations can be sufficiently pronounced to span the limits of adiabatic and non-adiabatic behavior for a given redox pair.

Any polarized solvent surrounding the encounter complexes dealt with in the present study is assumed to have a minor influence on H_{if} magnitudes, as supported by recent calculations [16] in which the supermolecule complex was placed in a cavity within a polarized continuum.

2. THEORETICAL AND COMPUTATIONAL DETAILS

2.1. Kinetic Model

In order to establish a concrete link between the rate constant for electron transfer, k_{et}, and the electron transfer matrix element, H_{if}, we consider the following generalized transition state theory (TST) expression [2,6c]:

$$k_{et}^{TST} = (K_{pre\text{-}eq})(\exp[-\beta E^{+}])(\nu_n \kappa_{e\ell}) \tag{3}$$

where the three factors in parentheses correspond respectively to the formation of the precursor complex (K is the pre-equilibrium constant), the activation of the precursor complex, and the passage from initial to final state at the transition state. Our interest in the present work lies in the attenuation of the rate of the latter process due to the electronic transmission coefficient $\kappa_{e\ell}$. With the help of the Landau-Zener model [18] we may represent $\kappa_{e\ell}$ as

$$\kappa_{e\ell} = 2P_o/(1+P_o) \tag{4}$$

where the probability P_o for hopping between diabatic surfaces, H_{ii} and H_{ff}, is given by

$$P_o = 1 - \exp(-2\pi\gamma) \tag{5}$$

and where, for a harmonic oscillator model,

$$2\pi\gamma = |H_{if}|^2 \, \pi^{3/2}/2h\nu_n(k_B T E^{\dagger})^{1/2} \tag{6}$$

In eq 5, ν_n is the harmonic frequency associated with the initial state (H_{ii}) and final state (H_{ff}) wells, and E^{+} is the activation energy (the energy at which H_{ii} and H_{ff} cross relative to the minimum of the H_{ii} well). Thus the magnitude of H_{if} is a crucial factor in determining where a given process lies relative to the non-adiabatic ($\kappa_{e\ell} \ll 1$) and adiabatic limits ($\kappa_{e\ell} \sim 1$). For typical activated electron processes, one is near the adiabatic limit when $|H_{if}| > k_BT$ at room temperature (i.e., ~ 200 cm^{-1}) [2].

2.2. Wavefunctions and Matrix Elements

The most straightforward approach to evaluating H_{if} (eq 2) is to obtain it directly, using calculated wavefunctions ψ_i and ψ_f [6a,7]. In general, ψ_i and ψ_f, which can be thought of as charge-localized valence bond structures, corresponding, respectively, to the left and right hand side of eq 1, are non-orthogonal ($S_{if} \equiv \int \psi_i\psi_f d\tau \neq 0$), As a result, eq 2 is generalized as follows:

$$H'_{if} = (H_{if} - S_{if}H_{ii})/(1 - S^2_{if}) \tag{7}$$

The states ψ_i and ψ_f are represented as single configuration (i.e., single determinant), wavefunctions and are determined variationally using the self-consistent field method (SCF) [6]. In previous studies of small model coordination complexes, we performed these calculations using <u>ab initio</u> methods. For the larger molecular complexes treated in the present study we have, for the most part, employed a version of the INDO method developed transition metal complexes by Zerner et al. [19]. In cases where comparison is possible, the <u>ab initio</u> and INDO approaches are found to yield comparable estimates of H'_{if} (generally within 20 or 30 percent of each other) [6c].

As an alternative to eq 6, in cases of symmetric electron exchange it is convenient to estimate H'_{if} values as the splittings of charge-delocalized state energies [6],

$$H'_{if} = (H^+ - H^-)/2 \tag{8}$$

where H^+ and H^- are the expectation values of the Hamiltonian with respect to the symmetric (+) and antisymmetric (-) charge-delocalized SCF wavefunctions, respectively. While the constraint of charge-localization suppresses a certain amount of electronic relaxation (a many-electron effect) relative to the fully-relaxed functions ψ_i and ψ_f, H'_{if} values obtained from eq 8 are generally quite close to those obtained from eq 7 [6c]. Most of the results presented below are based on eq 8, although comparisons with eq 7, are also included.

The method of corresponding orbitals [20] plays an important role not only in implementing eq 7, but also in casting the calculated results in a form which provides a straightforward definition of the effective donor and acceptor orbitals and allows a quantitative assessment of departures from a simple one-electron model for H'_{if}. The corresponding orbital transformations among the orbitals of the n-electron wavefunctions, ψ_i and ψ_f, define sets of n molecular orbitals, $\{\phi^i\}$ and $\{\phi^f\}$, respectively, which correspond maximally in pairs ($\phi_1{}^i$, $\phi_1{}^f$; $\phi_2{}^i$, $\phi_2{}^f$; ... $\phi_n{}^i$, $\phi_n{}^f$). A one-electron model is valid to the extent that a nearly invariant (n-1)-electron core can be identified ($\phi_k{}^i \sim \phi_k{}^f$, $k \leq n-1$), and the remaining pair of orbitals, $\phi_n{}^i$ and $\phi_n{}^f$, provide the natural definition of the donor acceptor orbitals [6c]. Departures from a purely one-electron model are identified with departures from unity of the overlap integrals, $S_k{}^{i,f} \equiv \int \phi_k{}^i \phi_k{}^f d\tau$, $k \leq n$.

For the $Co(NH_3)_6{}^{2+/3+}$ complexes, multiplet splittings were calculated from ab initio wavefunctions employing large basis sets (s,p,d, and f orbitals) and including electron correlation at the level of 2nd-order perturbation theory (MP2 [21]) relative to the SCF reference [14].

3. SUPEREXCHANGE COUPLING

3.1. The Role of Ligand Field Mixing

The role of ligand-field mixing in indirect superexchange coupling of metal-ion donor orbitals can be understood in terms of the following simplified scheme based on a single contact ligand-pair, in which the ligands are taken as electron donors (the case relevant to the water, ammine, and cyclopentadienide ligands considered below):

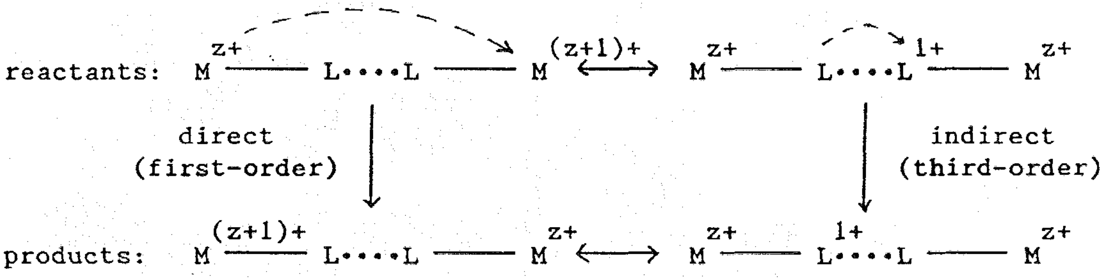

The reactant (ψ_i) and product (ψ_f) states are each represented as a resonance mixture of a primary valence bond structure (left-hand-side) and a valence structure corresponding to ligand-to-metal charge transfer (LMCT). Direct (first-order) electron transfer between metal ion sites (left-hand side) is of minor importance in comparison with indirect (third-order superexchange) electron transfer which exploits direct (first-order) coupling of adjacent ligands in conjunction with first order LMCT within each redox partner (right-hand side).

The above superexchange mechanism is of the "hole" type, involving electron-deficient virtual states of the intervening ligands [2]. For cases of electron-acceptor ligands, one would expect an analogous superexchange mechanism of the "electron" type in which the indirect donor/acceptor coupling is established via intervening electron-attachment states. The third-order "hole" mechanism for electron exchange between various aquo- and ammine complexes has been demonstrated quantitatively for encounter geometries with an apex-to-apex contact (i.e., a common four-fold axis), using ligand-field covalency parameters inferred from the calculated wavefunctions as a measure of the LMCT [6c].

3.2. Dependence of H'_{if} on Encounter Geometry

The magntidue of electron coupling by super-exchange of the type illustrated above will depend on the relative orientation of reactants in the encounter complex, since the nature of the ligand-ligand contacts will depend on the details of the encounter geometry. Thus for ligands involving peripheral hydrogen atoms, the primary contact may involve overlap of the hydrogen orbitals on the respective ligands, even in the case of π-type electron transfer, in which case the hydrogenic orbitals are coupled to the heavy atoms via hyper-conjugation. In addition, direct overlap between the orbitals of the heavy atoms of the ligands on the two reactants may be appreciable for certain orientations [6c]. On the other hand, one does not expect any particular correlation of overall coupling strength (and hence H'_{if} magnitude) with the distance between the nominal redox sites ($r_{MM'}$).

3.2.1. Hexa-aquo and Hexa-ammine Complexes. In Table 1 are displayed calcualted H'_{if} magnitude for three different encounter geometries, illustrating cases of both π-type (t_{2g}, $Fe(H_2O)_6{}^{2+/3+}$) and σ-type (e_g, $Co(NH_3)_6{}^{2+/3+}$) electron transfer. The selected geometries -- apex-to-apex, edge-to-edge, and face-to-face -- correspond to van-der-Waals contact between counter pairs sharing common four-fold, two-fold, and three-fold axes, respectively.

The H'_{if} values for π-electron transfer vary rather little inspite of appreciable changes in the number of ligand-ligand contacts and the metal-metal distance. The small increase which is observed in proceeding from the head-on apex-to-apex approach to the rather oblique ligand-ligand contacts in the edge-to-edge and face-to-face approaches probably reflects the increased role of direct overlap between reactant oxygen π orbitals (antisymmetric in the water planes) as the angle between FeO-FeO bonds in contact changes from 180° (apex-to-apex) to 90° (edge-to-edge and face-to-face) [6c].

The coupling for sigma electron transfer in the $Co(NH_3)_6{}^{2+/3+}$ system is both stronger and more sensitive to orientation than for the above case of π-electron transfer (a qualitatively similar conclusion was reached on the basis of extended Hückel calculations [8c,22]). Furthermore, the strong decrease of H'_{if} values is seen to occur even though the number of ligand-ligand contacts is increasing and the metal-metal separation is decreasing. The increased bulkiness of the NH_3 ligand relative to water leads to less variation in $r_{MM'}$ compared with that exhibited by the hexa-aquo complexes, and the directionality of the ammine lone pairs, leads to less effective direct inter-reactant overlap involving these orbitals than for the analogous case of the water pi-orbitals.

While all the displayed cases for $Fe(H_2O)_6{}^{2+/3+}$ correspond to an appreciable degree of non-adiabatic behavior ($\kappa_{e\ell} < 1$), the various $Co(NH_3)_6{}^{2+/3+}$ values are seen to span the range from weak adiabatic to strong adiabatic coupling. Of course, an overall assessment of the rate constant would require an estimate of the relative energies of the different precursor states in solution. For

TABLE 1. Orientation Dependence of H'_{if}

Orientation	H'_{if} $(cm^{-1})^a$	Number of L,L' Contacts	$r_{M,M'}$ (Å)
π/t_{2g} transfer $(FeH_2O)_6^{2+/3+}$			
apex-to-apex	18	1	7.4
edge-to-edge[b]	30	2	6.4
face-to-face	40[c]	6	5.3
σ/e_g transfer $(Co(NH_3)_6^{2+/3+}$			
apex-to-apex[d]	700	1	7.0
edge-to-edge[b]	120	2	6.9
face-to-face	80	6	5.8

a) Based on eq 8, using the lowest energy supermolecule states of g and u symmetry. For each of the three orientation, the redox partners are related by inversion through the symmetry center of the supermolecule complex. The geometrical parameters of the ML_6 complexes are the same as those given in ref. [6].

b) The adjacent "octahedral edges" are parallel.

c) A very similar result ($38\ cm^{-1}$) was obtained using eq 7.

d) The process involves an excited spin state (^2E_g; t_{2g}^6/e_g); this state is coupled to the ground state ($^4T_{1g}$; t_{2g}^5/e_g^2) by spin-orbit mixing, as discussed in Section 3.3.

$Fe(H_2O)_6^{2+/3+}$ the face-to-face approach is likely to be dominant [23,24].

3.2.2. Metallocene Systems. We turn now from the saturated H_2O and NH_3 ligands to the unsaturated cyclopentadienide (Cp^-) ligand. When a metallocene (Cp_2M) is ionized to form the metallocinium ion (Cp_2M^{1+}), the hole formed in one of the metal d-orbitals is strongly screened by LMCT into the vacancies in the other 3d orbitals [19a]. Accordingly, it is of interest to investigate the effect of such screening on H'_{if} values for metallocene/metallocinium redox pairs, especially since experimental estimates of H'_{if} have been obtained by Weaver et al. for the cases M = Fe and Co [25]. Theoretical and experimental results are presented in Table 2.

The Fe and Co results offer an interesting comparison since the transferred electron in the case of Fe has "delta" symmetry (i.e., transforming as x^2-y^2, or xy, where the reference direction is the five-fold symmetric z-axis), while the analogous symmetry for Co is "pi" (transforming as xz or yz). Thus for cobaltocene, we expect better metal-ligand overlap, and hence, more delocalization in the effective donor and acceptor orbitals.

The data in Table 2 are presented in order of increasing interreactant coupling, and include coaxial (D_{5h}) and side-by-side (D_{2h}) approaches, as well as an intermediate (C_{2h}) structure. We have also included the covalently-bound bi-metallocene system [27]. As in Table 1, we find no apparent correlation between H'_{if} and

TABLE 2. H'_{if} Values for Metallocene Redox Pairs (cm^{-1})^{a}

Structure	M = Fe^{b} calc^{d}	M = Fe^{b} exp	M = Co^{c} calc^{d}	M = Co^{c} exp	$r_{MM'}$ (Å)
(D_{2h}) 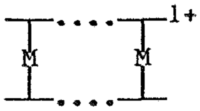	20	35^{e}	40	175^{e}	5.92
(C_{2h}) 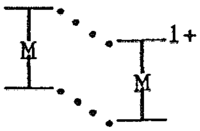	50		350		5.29
(D_{5h}) 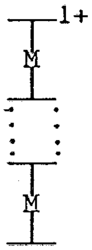	140		870		6.58
(C_{2h}) 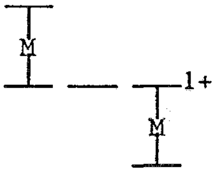	1050	$\gtrsim$ 500^{f}	2240	$\gtrsim$ 1100^{f}	5.14

a) $(CpMCp)^{0/1+}$ redox pairs, where Cp $\equiv$ C_5H_5. In the present model studies, a common geometry was used for all metallocene species: D_{5h} symmetry; r_{cc} = 1.42 Å; r_{CM} = 1.62 Å; r_{CH} = 1.10 Å. Experimental geometrical data and pertinent references are summarized by Weaver et al. [26]. The first three structures represent van-der-Waals contact (edge-to-edge, with H•••H ~ 2.2 Å for D_{2h}, C_{2h}), and C•••C = 3.5 Å for D_{2h}). In the last case (bimetallocene), the metallocenes are linked by a single covalent bond (r_{cc} = 1.64 Å). For D_{2h} and C_{2h} cases, results pertain to lower energy component of split degenerate states (see footnote a, Table 3).

b) The zeroth-order picture of the ferrocinium cation involves removal of a 3dδ electron (defined with respect to the five-fold σ axis of the metallocene).

c) The zeroth order picture of the cobaltocinium cation involves removal of a 3dπ electron (defined as in footnote b).

d) Calculated using eq 8.

e) Ref. [25].

f) Obtained as lower limits from analysis of intervalence charge-transfer spectra [27].

$r_{MM'}$, and once again, the orientational variation is seen to span the range from non-adiabatic to strong adiabatic coupling. The theoretical values for the non-bonded metallocene-metallocinium contact pairs bracket the experimental estimates [25], while the theoretical values for the bi-metallocene systems, assuming trans conformations, are consistent with the experimental lower limits [27]. More precise contact with experiment will require estimates of relative energies of the different structures.

The effect of electronic relaxation on H'_{if} is illustrated in Table 3 for the case of the C_{2h} encounter geometry. Relaxing the constraint of change-delocalization entailed in the use of eq 8 is seen to reduce H'_{if} magnitude by only 10-30%, and we thus find quantitative support for a one-electron model of the electron transfer process. The details of the calculations also reveal that non-unit overlap factors associated with the n-1 electron core (see Section 2) attenuate the one-electron contribution to H'_{if} in the localized representation (eq 7) by only 10%, thus providing further support for the one-electron model. The effective donor and acceptor orbitals in this model are found from the corresponding orbital analysis to be primarily localized on the metal atom (~ 75%) for the case of Fe, while for Co the orbitals are about evenly shared by metal and ligands.

The robustness of the one-electron model, as assessed by the preceding criteria, is maintained in spite of the appreciable screening (an intrinsically many-electron effect) which accompanies the ionization of metallocenes, as noted above. For both ferrocene and cobaltocene, more than 70% of the d-orbital depletion of the donor molecular orbital is screened by LMCT involving the other molecular orbitals.

TABLE 3. Effect of Relaxation on H'_{if} (cm^{-1})[a]

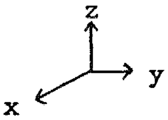		Fe[b]			Co[c]	
		deloc[d]	loc[e]		deloc[d]	loc[e]
(C_{2h}) 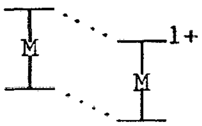	xy	50	35	yz	350	280
	x^2-y^2	13	10	xz	40	35

a) The 2-fold degeneracy associated with the metallocene five-fold axis is broken in the encounter complex. The first row of H'_{if} values refers to the lower-energy component in each case (xy and yz symmetry, respectively, for the donor/acceptor orbitals in the Fe and Co systems).
b) See footnote b, Table 2.
c) See footnote c, Table 2.
d) Calculated using eq 8.
e) Calculated using eq 7.

3.3 A Role for Spin-Orbit Coupling

Situations may arise in which ground-state spin multiplets do not by themselves serve as useful localized donor and acceptor states in superexchange schemes of the type considered above. Such a situation may well pertain to the cease of the $Co(NH_3)_6{}^{2+/3+}$ exchange process [13,14]. As indicated in the following scheme,

$$Co(NH_3)_6{}^{2+} + Co(NH_3)_6{}^{3+} \longrightarrow Co(NH_3)_6{}^{3+} + Co(NH_3)_6{}^{2+}$$

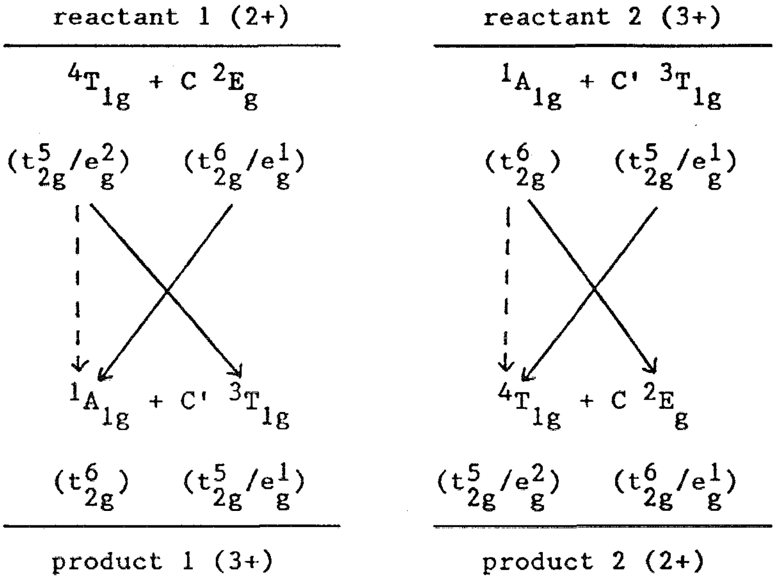

the pathway connecting ground spin states (dashed vertical arrows) is formally a "three-electron" process (inter-reactant transfer of an electron and an $e_g \leftrightarrow t_{2g}$ rearrangement within each redox partner) and is thus expected to have very low probability.

On the other hand, the observed reaction in aqueous solution exhibits "normal" electron transfer kinetics [28] based on the Marcus transition state model [1], thus appearing to rule out the existence of an unusually small $\kappa_{e\ell}$ factor. Accordingly we are led to consider various "one-electron" pathways (solid diagonal arrows) which become accessible to the extent that spin-orbit coupling occurs in the ground state species. It is these one-electron pathways which are governed by the LMCT-driven superexchange mechanism illustrated in Section 3.2.1, but the overall superexchange process here will be higher order (formally fifth order) since first-order spin-orbit coupling is required in each reaction partner.

A critical ingredient for perturbatively estimating the strength of the spin-orbit coupling is the high-spin/low-spin energy splitting for the 2+ and 3+ ions. While the value for the 3+ ion is known from spectroscopy [29], the most likely smaller, and hence more important, value for the 2+ ion is not available experimentally, although INDO calculations [22] have suggested that it may be quite small (< 5000 cm^{-1}). Accordingly, we have attempted to calculate this quantity [14], using correlated electronic structure techniques with very large basis sets (see section 2), and empirically correcting the calculated splitting by exploiting the close analogy between the electronic state differences for the two different charge states: i.e., for each charge state the low-spin → high-spin process corresponds to the breaking of a t_{2g}^2 pair accompanied by a $t_{2g} \rightarrow e_g$ excitation. The sensitivity of the calculated splittings to various levels of calculation is indicated in Table 4.

TABLE 4. Sensitivity of Calculated high-spin/low-spin energy splittings [14], (ΔE^{z+}, 10^3 cm^{-1})

$$\Delta E^{3+} \equiv E(^3T_{1g}) - E(^1A_{1g})$$
$$\Delta E^{2+} \equiv E(^2E_g) - E(^4T_{1g})$$

Computational Level	ΔE^{3+} a	ΔE^{2+} a
SCF	1.2	16.2
2nd-order correlation (MP2)b		
s,p,d basis	---	13.9
s,p,d,f basisc	7.7	12.4
empirically correctedc,d	13.7	6.4

a) Based on calculated equilibrium Co-N bond lengths: 2.07 Å(3+) and 2.29 Å(2+).
b) Ref. [21].
c) Includes basis functions of _f_ symmetry on Co.
d) The positive correction term, E_{corr}, which brings the 3+ value into exact agreement with the known experimental value [29], was also employed to correct the 2+ value. Given the definitions of ΔE^{2+}, the correction of ΔE^{3+} by $+E_{corr}$ implies correction of ΔE^{2+} by $-E_{corr}$.

Table 5 reveals that for the geometry most pertinent to the kinetics (i.e., the transition state value of the Co-N bond length), the splittings are significantly less than for the respective equilibrium geometries, and hence the spin-orbit coupling is expected to be correspondingly greater. Using atomic ion values for the necessary spin-orbit matrix elements, we finally obtain [14] estimates of ~ 0.10 and ~ 0.30 for the spin-orbit mixing coefficients in the two low lying states of the 2+ ion, and ~ 0.15 for the 3+ ion (these are the coefficients C,C' in the above scheme.

Applying these results to the case of the apex-to-apex approach of reactants, we obtain an effective H'_{if} value of ~ 25 cm^{-1} (scaling the "one-electron" H'_{if} value of 700 cm^{-1} listed in Table 1 by a spin orbit attenuation factor of ~ 0.03) and hence via (eqs 4-6) an overall $\kappa_{e\ell}$ value of ~ 10^{-2}. Thus the spin-orbit

TABLE 5. Variation of ΔE^{2+} values with Co-N bond length[a]

species	equilibrium		transition state	
	r_{CoN} (Å)	$\Delta E(10^3\ cm^{-1})$	r_{CoN}(Å)	$\Delta E(10^3\ cm^{-1})$
3+ ion	2.07	13.7	2.15	10.0
2+ ion	2.29	6.4	2.15	2.2

a) All ΔE value have been corrected (last entry in Table 4). The following general linear relationships have been obtained [14]: $\Delta E^{3+} = 109.3 - 46.2\ r_{CoN}$ and ΔE^{2+} - $-61.6 + 29.7\ r_{CoN}$. The calculated r_{CoN} values are uniformly about 0.1 Å larger than the experimental values. Compensation for errors in calculated ΔE values arising from the systematic shift of bond lengths is included in the empirical correction (see Table 4).

coupling mechanism seems capable of accounting for the absence of very strong departures from the adiabatic limit in the observed kinetics [28]. Further calculations suggest that the activation energy for the spin-orbit ground state pathway is somewhat smaller than that for the pathway involving the thermally excited ^2E state of $Co(NH_3)_6{}^{2+}$ [30].

As a final comment it is worth noting that the sensitivity of high-spin/low-spin splitting energies to variations in r_{CoN} (Table 5) implies a corresponding variation in the H'_{if} value along the reaction coordinate (since the r_{CoN} values control the inner-sphere component of this coordinate), and hence, an interesting departure from the Condon approximation [2].

4. SUMMARY

Electron transfer matrix elements for electron exchange between various pairs of transition metal complexes in close contact have been calculated and analyzed for a variety of approach geometries for the two reactants. The coupling between the nominal metal ion donor/acceptor sites is achieved by superexchange of the "hole" type arising from ligand-to-metal charge transfer (LMCT), the dominant ligand-field interaction for the electron-donor ligands considered (H_2O, NH_3, and the cyclopentadienide anion). The pronounced variations of H'_{if} with geometry are not correlated with the separation distance of the metal ions (between which the direct overlap is negligible) and span the range from non-adiabatic to strongly adiabatic electronic coupling. The values for metallocene/metallocinium redox pairs bracket recently reported experimental values. Analysis of the results using the method of corresponding orbitals demonstrates the validity of an effective 1-electron model for the electron transfer process to within about 10% for the class of systems considered. A higher-order superexchange mechanism was encountered for the $Co(NH_3)_6{}^{2+/3+}$ exchange process, in which the LMCT-driven hole-transport mechanism couples excited local states of the metal ions, which in turn are connected to the corresponding ground states by spin-orbit mixing. This mechanism yields on electronic transmission factor within two orders of magnitude of unity.

5. ACKNOWLEDGEMENT

This research was carried out at Brookhaven National Laboratory under contract DE-AC02-76CH00016 with the U.S. Department of Energy and supported by its Division of Chemical Sciences, Office of Basic Energy Sciences.

6. REFERENCES

1. (a) Marcus, R. A. J. Chem. Phys. (1956) **24**, 966; (b) 1956, **24**, 979.
2. Newton, M. D.; Sutin, N. Ann. Rev. Phys. Chem. (1984) **35**, 437-480.
3. Calef, D. F.; Wolynes, P. G. J. Phys. Chem. (1983) **87**, 3387-3400.
4. Hynes, J. T. J. Phys. Chem. (1986) **90**, 3701-3706.
5. Marcus, R. A.; Sutin, N. Biochim. Biophys. Acta (1985) **811**, 265-322.
6. (a) Logan, J.; Newton, M. D. J. Chem. Phys. (1983) **78**, 4086; (b) Newton, M. D. J. Phys. Chem. (1988) **92**, 3049; (c) Newton, M. D. J. Phys. Chem. (1988) **92**, 3049.
7. Ohta, K.; Closs, G. L.; Morokuma, K.; Green, N. J. J. Am. Chem. Soc. (1986) **108**, 1319-1320; Ohta, K.; Morokuma, K. J. Phys. Chem. (1987) **91**, 401.
8. (a) Larsson, S. J. Am. Chem. Soc. (1981) **103**, 4034; (b) Larsson, S. J. Chem. Soc. Faraday Trans. (1983) **279**, 1375-1388; (c) Larsson, S. J. Phys. Chem. (1984) **88**, 1321; (d) Larsson, S. Chemica Scripta (1988) **28A**, 15-20.
9. (a) Beratan, D. N.; Onuchic, J. N.; Hopfield, J. J. J. Chem. Phys. (1987) **86**, 4488; (b) Kuki, A.; Wolynes, P. Science (1987) **236**, 1647.
10. McConnell, H. M. J. Chem. Phys. (1961) **35**, 508.
11. Kuznetsov, A. M.; Ulstrup, J. J. Chem. Phys. (1981) **75**, 2047.
12. Goodenough, J. B. (1963) Magnetism and the Chemical Bond, John Wiley & Sons, New York.
13. Buhks, E.; Bixon, M.; Jortner, J.; Navon, G. Inorg. Chem. (1979) **18**, 2014.
14. Newton, M. D. ACS Symp. Ser., in press.
15. Plato, M.; Möbius, K.; Michel-Beyerle, M. E.; Bixon, M.; Jortner, J. J. Am. Chem. Soc. (1988) **110**, 7279-7285.
16. Scherer, P. O. J.; Fischer, S. F. J. Phys. Chem. (1989) **93**, 1633-1637.
17. Mikkelsen, K. V.; Dalgaard, E.; Swanst0m, P. J. Phys. Chem. (1987) **91**, 3081-3092.

18. Landau, L.; Phys. Z. Sowjet. (1932) **2**, 46; Zener, C. Proc. Roy. Soc. London (1932) **Ser. A**, 696.
19. (a) Zerner, M. C.; Loew, G. H.; Kirchner, R. F.; Mueller-Westerhoff, U. T. J. Am. Chem. Soc. (1980) **102**, 589; (b) Anderson, W. P.; Edwards, W. D.; Zerner, M. C. Inorg. Chem. (1986) **25**, 2728-2732.
20. King, H. F.; Stanton, R. E.; Kim, H.; Wyatt, R. E.; Parr, R. G. J. Chem. Phys. (1967) **47**, 1936.
21. Krishnan, R.; Firsch, M. J.; Pople, J. A. J. Chem. Phys. (1980) **72**, 4244.
22. Larsson, S.; Stahl, K.; Zerner, M. C. Inorg. Chem. (1986) **25**, 3033-3037.
23. (a)Tembe, B. L.; Friedman, H. L.; Newton, M. D. J. Chem. Phys. (1982) **76**, 1490; (b) Friedman, H. L.; Newton, M. D. Faraday Discuss. Chem. Soc. (1982) **74**, 73-81.
24. Kuharski, R. A.; Bader, J. S.; Chandler, D.; Sprik, M.; Klein, M. L. J. Chem. Phys. (1988) 89, 3248-3257.
25. Weaver, M. J.; Gennett, T. Chem. Phys. Lett. (1985) **113**, 213; Gennett, T.; Milner, D. F.; Weaver, M. J. J. Phys. Chem. (1985) **89**, 2787-2794.
26. McManis, G. E.; Nielson, R. M.; Gochev, A.; Weaver, M. J. J. Am. Chem. Soc. (1989) in press.
27. McManis, G. E.; Nielson, R. M.; Weaver, M. J. Inorg. Chem. (1988) **27**, 1827-1829.
28. Hammershoi, A.; Geselowitz, D.; Taube, H. Inorg. Chem. (1984) **23**, 979.
29. Wilson, R. B.; Solomon, E. I. J. Am. Chem. Soc. (1980) **102**, 4085.
30. Newton, M. D., to be published.